Measurement Uncertainty Analysis of an Accelerometer Calibration Using a POC Electromagnetic Launcher

E. J. Timpson P.E., T. G. Engel Ph. D.
Department of Electrical and Computer Engineering, University of Missouri, Columbia, MO,
etimpson@kcp.com

Abstract — **A pulse forming network (PFN), helical electromagnetic launcher (HEML), command module (CM), and calibration table (CT) were built and evaluated for the combined ability to calibrate an accelerometer. The PFN has a maximum stored energy of 19.25 kJ bank and is fired by a silicon controlled rectifier (SCR), with appropriate safety precautions. The HEML is constructed out of G-10 fiberglass reinforced epoxy and is designed to accelerate a mass of 600 grams to a velocity of 10 meters per second. The CM is microcontroller-based running Arduino Software. The CM has a keypad input and 7 segment outputs of the PFN voltage and desired charging voltage. After entering a desired PFN voltage, the CM controls the charging of the PFN. When the two voltages are equal it sends a pulse to the SCR to fire the PFN and in turn, the HEML. The HEML projectile's tip hits a target that is held by the CT. The CT consists of a table to hold the PFN and HEML, a vacuum chuck, air bearing, velocimeter and catch pot. The target is held with the vacuum chuck awaiting impact. After impact, the air bearing allows the target to fall freely so that the velocimeter can accurately read. A known acceleration is determined from the known change in velocity of the target. Thus, if an accelerometer was attached to the target, the measured value can be compared to the known value.**

I. Introduction and Background

The US Department of Defense has considered electromagnetic launchers for weapons and other applications. In 2010, NASA released press that they were studying electric launchers for the first part of a journey to the stars. Helical launchers are the most promising of all types of electromagnetic launchers in terms of efficiency. This paper marks the first industry application of a helical electromagnetic launcher (HEML) – the calibration of an accelerometer. Electromagnetic launchers are ideal for repeatability, controllability, high accelerations, velocities, and short travel requirements.

Accelerometers are calibrated with a number of processes. The process presented in this paper is common but with a different method for actuation - HEMLs. Other methods of actuation include elastics added gravity, pneumatics, and chemicals. All of which have some advantages. This work compares those advantages with electromagnetic launchers.

A. Electromagnetic Launchers

Over the years there has been considerable attention given to electromagnetic launchers. The major advantage of electromagnetic propulsion, at least for anti-armor mission, is the ability to reach higher impact velocities [1]. Higher velocities are important for many applications. For launching to Space with an electromagnetic gun Ian McNab said, "These techniques have the advantage that the launch mechanism remains on the Earth and does not have to be lifted into space, as with a rocket." [2] In the same paper he reviews gun options including electromagnetic rail guns, EM coilguns, electrothermal-chemical guns, light gas guns, RAM accelerators, blast wave accelerators, slingatron, and even lasers. In the end, because the government spent money and time on railguns, he chooses railguns. One year later, efficiency and scaling relationships for DC (i.e. non-induction) electromagnetic launchers opened a new door [3]. The exploration continued and formed a body of evidence [4-5]. Based on this evidence, the obvious choice is a HEML.

The HEML used in this paper operates in the same way as described in Reference [6]. Reference [7] shows further progress in the art of making a HEML, specifically with the variable inductive gradient. The HEML in this paper does not use the variable inductive gradient as it operates at relatively low velocities which make it difficult to implement a suitable variable inductance gradient scheme.

B. Calibration of Accelerometers

There are two primary domains with regard to acceleration: magnitude and duration. The two are interrelated; however, calibration methods typically explore variations of each, independent of one another. Specifically, duration is evaluated with a shaker at many frequencies (e.g., 2Hz to 10kHz) and constant amplitude (e.g., 10 g). We compared the test accelerometer to a Standard Accelerometer (Figure 1). The sensitivity derived from the vibration data

helps in evaluating amplitude. Amplitude can be evaluated by using a reference accelerometer (i.e. Back to Back). Amplitude can also be evaluated by comparing with velocity change (i.e. the absolute method of calibration). The following is a step by step procedure of evaluating amplitude variation using the absolute method:

Step 1 – Attach accelerometer to the target.

SNAM24 Endevco 2271AM20 Accelerometer Date: 1/24/11

The accelerometer was calibrated at the National Institute of Standards and Technology (NIST) on November 10, 2010. The certification is based on the average of the current NIST "Report of Test," NIST Test No. 681/280134-11, END297, and its history. The accelerometer is certified as follows:

Nominal g-level (g)	Frequency (Hz)	Sensitivity (pC/g)	Uncertainty (±%)
0.2	2	12.10	2
0.5	5	12.07	2
1	10	12.06	2
1	20	12.03	2
1	30	12.01	2
1	50	12.01	2
10	100	12.00	1
10	300	11.98	1
10	500	11.99	1
10	1000	11.99	1
10	2000	12.05	1
10	3000	12.15	2
10	4000	12.31	2
10	5000	12.54	2
10	6000	12.81	2
10	7000	13.06	2
10	8000	13.43	2
10	9000	13.89	2
10	10000	14.43	2

Note: The uncertainties listed above are an expanded uncertainty with a coverage factor k=2.

Figure 1. Standard accelerometer certification.

Step 2 – Turn on vacuum chuck and air bearing.

Step 3 – Place target (with accelerometer attached) in the vacuum chuck air bearing assembly (Figure 2).

Step 4 – Ensure computer software, counter, and oscilloscope are ready to acquire data.

Step 5 – Deliver shock – actuation.

Step 6 – Analyze data. Compare accelerometer readout with velocity change information to acquire sensitivity.

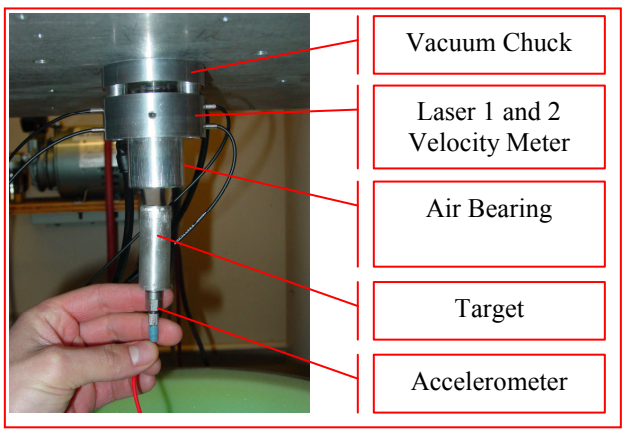

Figure 2. Accelerometer Calibration Setup Below the Table.

Traditionally, actuation takes place by bungee cord and bow release.

II. System Design

A new system was developed using an electromagnetic launcher as the actuator. The calibration table (CT) and in turn the calibration uncertainty is based off of the well know methods discussed in the introduction. The CT consists of a table to hold the pulse forming network (PFN) and HEML. Attached to the bottom of the CT are a vacuum chuck, air bearing, and laser velocity meter. Below the CT is a catch pot (Figure 3 – green foam filled pot).

Figure 3. Entire system

The command module (CM) was built new for this application. In an effort to get the same pull-it-back-and-let-it-go operation, simplicity was the driving factor. An Arduino microcontroller is the heart of the Proof of Concept CM. The microcontroller communicates with the user by seven segment displays (and other LEDs). The user communicates with the microcontroller with a keypad and Fire button. One can see the CM in Figure 3 as the black box on the CT. The CM's job is to monitor and control the PFN. This includes: 1) Monitor safety switches (including an emergency stop) for human exposure to High voltage and immediately discharge the capacitors if energized. 2) Await the desired bank Voltage from the user. 3) Upon obtaining confirmation from the user, the CM charges the Capacitor Bank to the Desired Voltage (with a High Voltage Power supply) 4) The CM stops charging at the desired voltage. 5) The CM awaits user input to fire the HEML and upon receiving this input discharges the capacitors into the HEML.

As mentioned, Reference 6 contains a detailed description of the HEML, its operating principles and equations. In short, the HEML is comprised of a barrel and projectile. One can see the barrel in Figure 3 (a green tube at a slant to expose the shiny projectile tip). The barrel is essentially a coil of wire with two insolated rails for providing current to the projectile. The projectile (Figure 4) is essentially another coil of wire with contacts to the rails and barrel coil. Current flows from one rail through the two coils of wires (barrel and projectile) to the other rail. Large current through the two coils creates two large opposing magnetic fields. The

opposition accelerates the projectile, allowing the tool hardened steel tip to contact the Target through a hole in the CT.

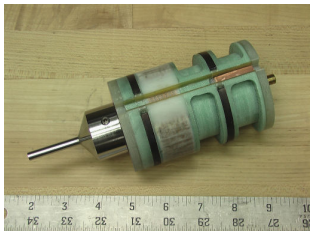

Figure 4. HEML projectile with tool hardened tip

A. Calibration and Experiment

Figure 5 illustrates the sequence of events. Figure 6 describes the variables in Figure 5.

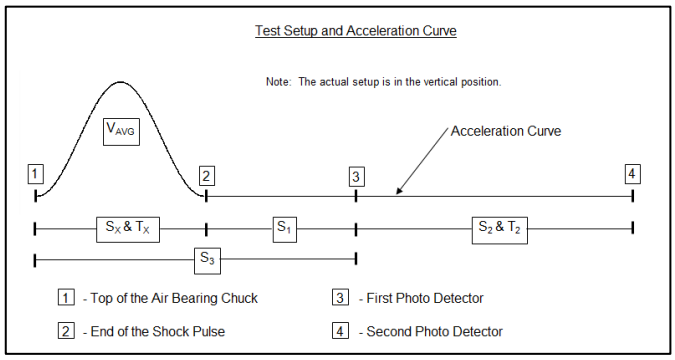

Figure 5. Test Setup and Acceleration Curve

S_X - Distance from the beginning to the end of the shock pulse
S_1 - Distance traveled from the end of the pulse to the first photodetector
S_2 - Distance traveled from the first photo detector to the second photo detector
S_3 - Distance from the top of the air bearing chuck to the first photo detector
T_X - Time taken for the accelerometer/anvil to travel from the beginning to the end of the shock pulse
T_2 - Time taken for the accelerometer/anvil to travel from the first photo detector to the second photo detector
V_1 - Velocity at position 1 is the initial velocity; accelerometer/anvil at rest, so $V_1 = 0$
V_2 - Velocity at position 2, the end of the shock pulse
V_3 - Velocity at position 3, the first photo detector
V_4 - Velocity at position 4, the second photo detector
V_{AVG} - Average velocity between position 1 and position 2.
g_1 - Acceleration of gravity for FM&T (g=386.0885827 in/s^2 and g_1 = 385.815 in/s^2)

Figure 6. Definition of variables.

Figure 7 illustrates a collection of equations that are derived from basic Physics and Figure 5.

Equations

(1) $V_4 = V_3 + g_1 \times T_2$

(2) $V_4^2 = V_3^2 + 2 \times g_1 \times S_2$

(3) $V_3^2 = V_2^2 + 2 \times g_1 \times S_1$

(4) $V_{AVG} = \frac{(V_1 + V_2)}{2}$

(5) $S_X = T_X \times V_{AVG}$

(6) $S_3 = S_1 + S_X$

Figure 7. Equation Collection

The calibration parameter is sensitivity (e.g., 0.1 mV per g). The sensitivity is calculated using Equation 7.

$$SC = (g_1 \times A \times SF) / V_2 \quad (7)$$

g_1 - Acceleration of gravity for FM&T
A - Area under the shock pulse
SF - Signal conditioning scale factor
V_2 - Velocity change

Gravity (g_1) is in Figure 6. Area under the shock pulse (A) is taken off the oscilloscope integrating function (It also equals V_s *T_s, or pulse width times the amplitude). The signal conditioning Scale Factor (SF) is one because the accelerometer under test used a signal conditioner (vs a capacitor or charge amplifier). Velocity change (V_2) is the change in velocity from position 1 to position 2. The velocity at position 1 is 0, so the velocity change is the velocity at position 2. S_2 and T_2 are measured quantities so starting with equation (1) or (2) will lead us to the calculation of V_2. Here we use equation (1). Let V_4 = ds/dt, solve for ds and integrate:

$$\frac{ds}{dt} = V_3 + g_1 \times T_2 \quad (8)$$

$$ds = (V_3 + g_1 \times T_2) \times dt \quad (9)$$

$$\int_0^{S_2} ds = \int_0^{T_2} (V_3 + g_1 \times T_2) dt \quad (10)$$

$$S_2 = V_3 \times T_2 + \frac{1}{2} \times g_1 \times T_2^2 \quad (11)$$

Solve for V_3

$$V_3 = \frac{S_2}{T_2} - \frac{1}{2} \times g_1 \times T_2 \quad (12)$$

Substitute Equation (12) into Equation (3) and solve for V_2:

$$V_2 = \sqrt{\left(\frac{S_2}{T_2} - \frac{1}{2} \times g_1 \times T_2 \right)^2 - 2 \times g_1 \times S_1} \quad (13)$$

Note: Equation (13) is in Reference [10] on page 146.
Solve Equation (4) for V_{AVG} when V_1 is zero.

$$V_{AVG} = \frac{V_2}{2} \quad (14)$$

Substitute V_{AVG} into Equation (5)

$$S_X = \frac{1}{2} \times T_X \times V_2 \quad (15)$$

Solve Equation (6) for S_x, substitute into Equation (9), and solve for S_1

$$S_1 = S_3 - \frac{1}{2} \times T_X \times V_2 \quad (16)$$

Substitute Equation (10) into Equation (8) and solve for V_2.

$$V_2^2 + \left(-g_1 \times T_X\right) \times V_2 + \left[2 \times g_1 \times S_3 - \left(\frac{S_2}{T_2} - \frac{1}{2} \times g_1 \times T_2\right)^2\right] = 0 \quad (17)$$

Using the quadratic formula and that the negative solution is less than zero and V_2 cannot be less than zero, the V_2 solution is as follows:

$$V_2 = \frac{1}{2} \times g_1 \times T_X + \sqrt{\frac{S_2^2}{T_2^2} - 2 \times g_1 \times S_3 - g_1 \times S_2 + \frac{1}{4} \times g_1^2 \times T_X^2 + \frac{1}{4} \times g_1^2 \times T_2^2} \quad (18)$$

Equation (18) is in the calibration software. The calibration software also talks to the counter and oscilloscope using GPIB.

The experiment was to calibrate the same accelerometer using the bungee cord and bow release method, and compare that to the new HEML method.

B. Uncertainty Evaluation

We used the NIST GUM method to construct the Uncertainty Analysis [11]. We shall start by defining all uncertainties in Figure 8.

dS_2 - Type B uncertainty for Air Bearing Chuck distance between the two photo detectors used in the Velocity calculations

dT_2 - Type B uncertainty for Standard Counter's time measured between the two photo detectors used in the Velocity calculations.

dS_3 - Type B uncertainty for Air Bearing Chuck distance between top and first photo detector used in the Velocity calculations.

dT_S - Type B uncertainty for the Standard Oscilloscope time measurements used in the Area calculations.

dT_X - Type B uncertainty for the Standard Oscilloscope time measurements used in the Velocity calculations.

dV_S - Type B uncertainty for the Standard Oscilloscope amplitude measurements used in the Area calculations.

dE_1 - Type B uncertainty for the Standard Oscilloscope amplitude measurements used in the Scale Factor calculations.

dE_0 - Type B uncertainty for the Standard AC Source amplitude used in the Scale Factor calculations.

dC - Type B uncertainty for the Standard Capacitor used in the Scale Factor calculations.

dg_1 - Type B uncertainty for the Acceleration of Gravity used in the Velocity calculations.

dSC_T - Type B uncertainty for room temperature variation of the accelerometers output.

dSC_F - Type B estimated uncertainty due to friction and tumbling as the anvil & accelerometer fall through the air bearing chuck.

dSC_V - Type B estimated uncertainty due to the vacuum suction holding the anvil & accelerometer in the air bearing chuck.

dSC_A - Type B estimated uncertainty due to the shock wave being transmitted through the anvil.

dSC_R - Type B estimated uncertainty due to accelerometer repeatabilty, reproducibility, and linearity.

dSC_O - Type B estimated uncertainty for miscellaneous excluded uncertainties.

dSC_C - Type B estimated uncertainty for calibration interval.

d - Uncertainty Divisor

k - Uncertainty coverage factor

Figure 8. Uncertainty Definitions

After defining all uncertainties, one must use partial differentials to determine the magnitude each has on the overall system. Equation (19) is the system equation (7) including the mathematical progress thus far.

$$SC = \frac{g_1 \times V_S \times T_S \times 1}{\frac{1}{2} \times g_1 \times T_X + \sqrt{\frac{S_2^2}{T_2^2} - 2 \times g_1 \times S_3 - g_1 \times S_2 + \frac{1}{4} \times g_1^2 \times T_X^2 + \frac{1}{4} \times g_1^2 \times T_2^2}} \quad (19)$$

In the interest of simplifying the differentials, new terms represent the numerator and the components of the denominator.

$$N_1 = g_1 \times V_S \times T_S \quad (20)$$

$$D_1 = \frac{1}{2} \times g_1 \times T_X \quad (21)$$

$$D_2 = \sqrt{\frac{S_2^2}{T_2^2} - 2 \times g_1 \times S_3 - g_1 \times S_2 + \frac{1}{4} \times g_1^2 \times T_X^2 + \frac{1}{4} \times g_1^2 \times T_2^2} \quad (22)$$

$$SC = \frac{N_1}{D_1 + D_2} \quad (23)$$

Now the Partial differentials follow:

$$\frac{\partial N_1}{\partial g_1} = V_S \times T_S = \frac{N_1}{g_1} \quad (24)$$

$$\frac{\partial N_1}{\partial V_S} = g_1 \times T_S = \frac{N_1}{V_S} \quad (25)$$

$$\frac{\partial N_1}{\partial T_S} = g_1 \times V_S = \frac{N_1}{T_S} \quad (26)$$

$$\frac{\partial D_1}{\partial g_1} = \frac{1}{2} \times T_X = \frac{D_1}{g_1} \quad (27)$$

$$\frac{\partial D_1}{\partial T_X} = \frac{1}{2} \times g_1 = \frac{D_1}{T_X} \quad (28)$$

$$\frac{\partial D_2}{\partial S_2} = \frac{2 \times S_2 - g_1 \times T_2^2}{2 \times D_2 \times T_2^2} \quad (29)$$

$$\frac{\partial D_2}{\partial S_3} = \frac{-g_1}{D_2} \quad (30)$$

$$\frac{\partial D_2}{\partial T_X} = \frac{g_1^2 \times T_X}{4 \times D_2} \quad (31)$$

$$\frac{\partial D_2}{\partial T_2} = \frac{-4 \times S_2^2 + g_1^2 \times T_2^4}{4 \times D_2 \times T_2^3} \tag{32}$$

$$\frac{\partial D_2}{\partial g_1} = \frac{-4 \times S_3 - 2 \times S_2 + g_1 \times T_X^2 + g_1 \times T_2^2}{4 \times D_2} \tag{33}$$

$$\frac{\partial SC}{\partial N_1} = \frac{1}{D_1 + D_2} = \frac{SC}{N_1} \tag{34}$$

$$\frac{\partial SC}{\partial D_1} = \frac{-N_1}{(D_1 + D_2)^2} \tag{35}$$

$$\frac{\partial SC}{\partial D_2} = \frac{-N_1}{(D_1 + D_2)^2} \tag{36}$$

Now we can combine using the RSS method.

$$dN_1 = \sqrt{\left(\frac{\partial N_1}{\partial g_1} \times dg_1\right)^2 + \left(\frac{\partial N_1}{\partial V_S} \times dV_S\right)^2 + \left(\frac{\partial N_1}{\partial T_S} \times dT_S\right)^2} \tag{37}$$

$$dD_1 = \sqrt{\left(\frac{\partial D_1}{\partial g_1} \times dg_1\right)^2 + \left(\frac{\partial D_1}{\partial T_X} \times dT_X\right)^2} \tag{38}$$

$$dD_2 = \sqrt{\left(\frac{\partial D_2}{\partial S_2} \times dS_2\right)^2 + \left(\frac{\partial D_2}{\partial T_2} \times dT_2\right)^2 + \left(\frac{\partial D_2}{\partial g_1} \times dg_1\right)^2 + \left(\frac{\partial D_2}{\partial S_3} \times dS_3\right)^2 + \left(\frac{\partial D_2}{\partial T_X} \times dT_X\right)^2} \tag{39}$$

$$dSC = \sqrt{\left(\frac{\partial SC}{\partial N_1} \times dN_1\right)^2 + \left(\frac{\partial SC}{\partial D_1} \times dD_1\right)^2 + \left(\frac{\partial SC}{\partial D_2} \times dD_2\right)^2} \tag{40}$$

It is seen that there are no correlation coefficients in the above equation. This paper is technically extended from the conference proceedings in that it contains the discussion of where this uncertainty is included [12]. The correlation is in the distance measurement.

The distance measurements are correlated due to the same instrument being used to measure both distances at the same time. This correlation is taken into consideration by increasing the uncertainty for both terms (i.e. dS_2 and dS_3). This result is a worst-case scenario, meaning it results in a higher uncertainty than if correlation coefficients are used.

III. Results

A. Calibration Results

Using the calibration procedure explained in Sections I and II, we calibrated an accelerometer using the old method and the new method. The accelerometer was a Kistler 8044 using a signal conditioner. The sensitivity was determined to be 0.1033 mV/g using the bungee cord method. The sensitivity was determined to be 0.1020 mV/g using the HEML method. For both methods the result of the uncertainty analysis is ± 2.83%. Figure 9 shows the shock pulse obtained with the new system. The amplitude was 11,432 g with a duration of 0.120 ms. The maximum bungee cord acceleration was 18,000 g at a pulse width of 0.100 ms. The highest acceleration recorded on the HEML system was 22,441 g at a pulse width of 0.1 ms. This was only operating at 400 volts or 3.08 kJ (not even 10% of the maximum capacity). The bungee cord method requires 42 centimeters of travel distance before hitting that target to get an acceleration of 18kg. The HEML operates at 2.54 cm independent of acceleration.

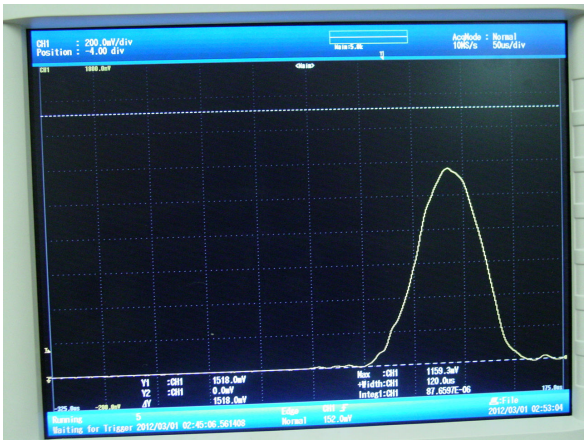

Figure 9. Calibration shock pulse (acceleration vs. time)

B. Comparison to other methods

The bungee cord method does have advantages. The largest advantage is simplicity; and because of that, timesaving (pull-it-back-and-let-it-go). Disadvantages to a bungee cord and bow release are operator dependence, large tower requirement for large amplitudes, and limitation on maximum acceleration. The HEML system has clear advantages over the bungee cord method in that it has no operator dependence; there is a considerable travel distance reduction, and no theoretical limit on velocity. The clear downside to the HEML launcher, because no PFN optimization has been done, is the increased time to operate.

Pneumatics also has advantages; in fact, the most popular actuation for high amplitude and frequency shock pulses is an air gun [8-9]. Air guns are not only physically larger, but the maximum velocity is limited by the speed of sound, whereas an electromagnetic launcher maximum velocity is not. It would be a wonderful future work to see a Hopkinson Bar operated with an electromagnetic launcher. Further one could

research from an energy storage perspective the cost of using an electric generator to fill up a tank (pneumatics) vs. the cost of directly charging the capacitors. In the case of power tools, especially ones used infrequently, there is a clear energy savings of electrics over pneumatics.

Chemical propellants have some advantages also. This work did not explore what specifically they would be; however, the clear downside to chemicals in comparison to electromagnetic launchers is the ease of repeatability with less cost in expendable materials. Using chemical propellants also requires licensed personnel and facilities.

IV. Conclusions

An electromagnetic launcher can calibrate an accelerometer. The HEML setup resulted in the same sensitivity as the bungee cord method. The HEML setup, operating at 16% of its maximum energy, exceeded the maximum acceleration of the old system. This work also suggests the exploration of electromagnetic launchers in a wide range of industry applications – specifically the calibration of accelerometers.

Acknowledgment

Gratitude is extended toward Matthew Clewell and Randy Herder for providing valuable contributions in many aspects of this work.

References

[1] Scanlon, J.J., III; Batteh, J.H.; Chryssomallis, G.; , "Tactical applications for electromagnetic launchers," *Magnetics, IEEE Transactions on* , vol.31, no.1, pp.552-557, Jan 1995 doi: 10.1109/20.364634 URL: http://ieeexplore.ieee.org/stamp/stamp.jsp?tp=&arnumber=364634&isnumber=8355

[2] McNab, I.R.; , "Launch to space with an electromagnetic railgun," *Magnetics, IEEE Transactions on* , vol.39, no.1, pp. 295- 304, Jan 2003 doi: 10.1109/TMAG.2002.805923 URL: http://ieeexplore.ieee.org/stamp/stamp.jsp?tp=&arnumber=1179826&isnumber=26497

[3] Engel, T.G.; Nunnally, W.C.; Gahl, J.M.; , "Efficiency and Scaling in DC Electromagnetic Launchers," *Pulsed Power Conference, 2005 IEEE* , vol., no., pp.249-252, 13-17 June 2005 doi: 10.1109/PPC.2005.300589 URL: http://ieeexplore.ieee.org.proxy.mul.missouri.edu/stamp/stamp.jsp?tp=&arnumber=4084199&isnumber=4084141

[4] Engel, T.G.; Neri, J.M.; Nunnally, W.C.; , "A Same-Scale Comparison of Electromagnetic Launchers," *Power Modulator Symposium, 2006. Conference Record of the 2006 Twenty-Seventh International* , vol., no., pp.405-410, 14-18 May 2006 doi: 10.1109/MODSYM.2006.365270 URL: http://ieeexplore.ieee.org.proxy.mul.missouri.edu/stamp/stamp.jsp?tp=&arnumber=4216222&isnumber=4216116

[5] Engel, T.G.; Veracka, M.J.; Neri, J.M.; , "The Specific-Force Performance Parameter for Electromagnetic Launchers," *Plasma Science, IEEE Transactions on* , vol.38, no.2, pp.194-198, Feb. 2010 doi: 10.1109/TPS.2009.2036260 URL: http://ieeexplore.ieee.org.proxy.mul.missouri.edu/stamp/stamp.jsp?tp=&arnumber=5342526&isnumber=5410033

[6] Engel, T.G.; Neri, J.M.; Veracka, M.J.; , "Solid-Projectile Helical Electromagnetic Launcher," *Plasma Science, IEEE Transactions on* , vol.37, no.4, pp.603-607, April 2009 doi: 10.1109/TPS.2009.2012714 URL: http://ieeexplore.ieee.org.proxy.mul.missouri.edu/stamp/stamp.jsp?tp=&arnumber=4776443&isnumber=4812340

[7] Engel, T.G.; Veracka, M.J.; , "Solid-Projectile Helical Electromagnetic Launcher With Variable Gradient Stator and Magnetically Levitated Armature," *Plasma Science, IEEE Transactions on* , vol.39, no.12, pp.3371-3377, Dec. 2011 doi: 10.1109/TPS.2011.2168570 URL: http://ieeexplore.ieee.org.proxy.mul.missouri.edu/stamp/stamp.jsp?tp=&arnumber=6036183&isnumber=6086645

[8] Bateman, V.I.; Leisher, W.B.; Brown, F.A.; Davie, N.T., "Calibration of a Hopkinson bar with a transfer standard," Presented at the 62nd Shock and Vibration Symposium, Springfield, VA, Oct. 1991

[9] Bateman, V.I.; Brown F.A.; Davie N.T., "Use of a Beryllium Hopkinson Bar To Characterize a Piezoresistive Accelerometer In Shock Environments," Journal of the Institute of Environmental Sciences, vol. 39, no. Nov. 1996

[10] Bouche, R.R., "Calibration of Shock and Vibration Measuring Transducers," Navel Research Laboratory, 1979, pp. 12 & 144-151, 1979

[11] Kuyatt, C.E.; Taylor, B.N., "Guide for Evaluating and Expressing the uncertainty of NIST Measuremet Results" NIST Technical Note 1297, 1994

[12] Timpson, E.J.; Engel T.G., "Calibrating Accelerometers Using an Electromagnetic Launcher" IEEE I2MTC 2012 conference proceeding.

This work has been funded by Honeywell Federal Manufacturing & Technologies under Contract No.DE-NA-0000622 with the U.S. Department of Energy. The United States Government retains and the publisher, by accepting the article for publication, acknowledges that the United States Government retains a nonexclusive, paid-up, irrevocable, world-wide license to publish or reproduce the published form of this manuscript, or allow others to do so, for United States Government purposes.